Micromechanics of fracture in nacre from mollusk shells

F. Barthelat and *R. Rabiei*
Department of Mechanical Engineering, McGill University, Montreal QC,
Canada

Nacre is the iridescent layer found inside many mollusk shells. This natural composite is mostly made of microscopic ceramic tablets bonded by a small fraction of organic materials. Nacre is 3,000 tougher that the ceramic it is made of, and its remarkable structure is now inspiring the design of novel biomimetic composites. The aim of this work is to characterize the microstructures and micromechanisms behind this remarkable performance. Deformation and fracture experiments were performed on millimeter size specimens from four types of nacres, using a miniature loading stage and in-situ microscopy. Nacre from pearl oyster showed to be the toughest of the nacres tested, with distinct and quite unusual deformation and fracture patterns. Microstructure-based finite element models are being developed in order to capture and quantify key microscale toughening mechanisms.

1 Introduction

Biomimetics, the science of mimicking nature in the design of novel artificial materials and systems, is becoming an important field that has started to yield materials with remarkable properties [1]. Nacre (mother-of-pearl) is a typical example of a high performance natural material which serves as model for next generation composites. Nacre is made of 95% vol. of the brittle aragonite, yet it is 3,000 tougher than that mineral. To this day this type of materials amplification is not matched by any manmade ceramic composite, and for this reason nacre has been investigated extensively over the past 30 years [2-6]. Nacre has a complex structure organized over several length scales (hierarchical structure). The main feature of this structure is a three dimensional brick wall like structure, with the "bricks" being microscopic aragonite polygonal tablets, and the "mortar" being a tough organic glue (Fig. 1a). Beyond this microscopic view of the structure of nacre, several nanoscale features are also present at the interface [4, 7] and also within the tablets [8, 9]. It is now widely accepted that the main deformation mechanisms of nacre is the microscale sliding of the tablets on one another (Fig. 1b). This mechanism enables relatively large deformations and energy dissipation by viscoplastic deformation of the softer interfaces [2, 6]. Additional toughening mechanisms include crack deflection, crack bridging by tablets and by resilient organic ligaments [10]. Since the remarkable structure and properties of nacre have been discovered, numerous "artificial nacres" have been produced using a wide range of fabrication techniques (see [11-13] for example). To this day,

however, none of these "artificial nacres" can duplicate the performance of natural nacre and its sliding mechanism. From these attempts it appears that it is not sufficient to produce microstructures that simply mimic some of the features of nacre. Microstructure optimization must enter the design of biomimetic materials in order to ensure that the proper deformation and failure mechanisms are achieved. In a recent article, Bonderer et al. have indeed used simple mechanistic models to optimize the aspect ratio of the inclusion, which led to a nacre like composite with unprecedented improvements [14]. The original, natural nacre itself is actually probably optimized for toughness [2, 15]. However there are several different nacre microstructures with different tablet arrangement, tablet thickness and aspect ratio [16] which suggest that there might be more than one optimum microstructure. In order to investigate the microstructure-performance relationships in nacre, deformation and toughness were investigated for nacre across four mollusk species. By comparing performances and how they relate to structure, it is hoped that one can gain deeper insight into the design and optimization of these materials.

| (a) | (b) |
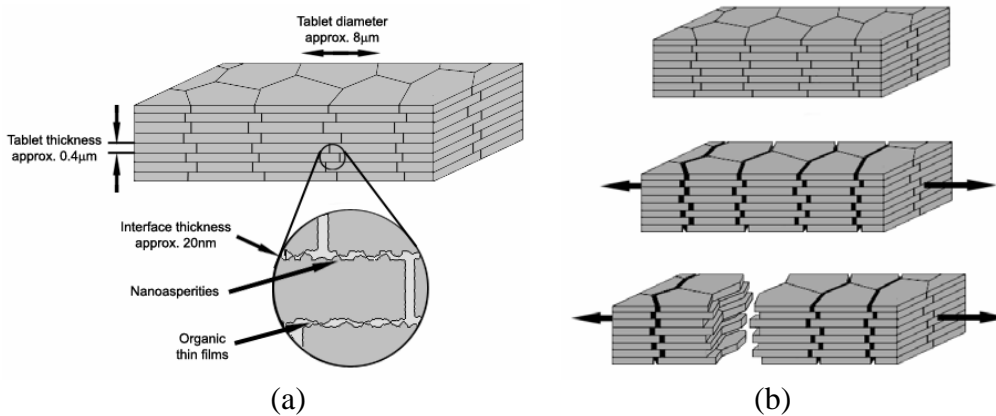
Figure 1: (a) Some key features of the structure of nacre; (b) the prominent deformation mechanism for nacre in tension: tablets sliding on one another.

2 Materials and Procedure

Four marine mollusk shells were selected for this study. They consisted of two gastropods: Red Abalone (*Haliotis Rufescens,* abbreviated RA) and Top Shell (*Trochus Niloticus,* TS) and two bivalves: Pen Shell (*Pinna Nobilis,* PS) and Pearl Oyster (*Pinctada Margaritifera,* PO). All nacreous shells consisted of an outside calcitic layer, and of an inner nacreous layer. The thickness of the shell varied significantly from species to species, ranging from about 10 mm for red abalone down to about 1 mm for Pen shell. The microstructure of the nacreous layer from these shells also differed. Nacre from the two gastropods has a columnar arrangement (the tablets are arranged in columns), whereas nacre for the two bivalve species has a more random arrangement (sheet nacre). The size and aspect ratio of the tablets also varied significantly from species to species (Fig. 2).

Specimen preparation started by sawing small plates from the shell. The calcite layer was removed and the two faces of the plate were made flat and parallel using a milling machine at low speed and using water coolant. 20 mm long bars were then cut from that plate using a precision diamond saw. The cross section varied from species to species, ranging from 0.2 mm by 0.5 mm to 1 mm by 1 mm. The specimens were stored in water prior to testing. All mechanical experiment were performed in four point bending configuration on a miniature mechanical loading stage (Fullam, Clifton Park NY) placed under an upright metallographic microscope (Olympus Canada, Markham, ON). For the deformation test, the surface of the specimen was lightly scratched with the tip of a needle in order to generate dark and light features (Fig. 3a). These features were used to determine displacements and strains from one image to the next using digital image correlation [17].
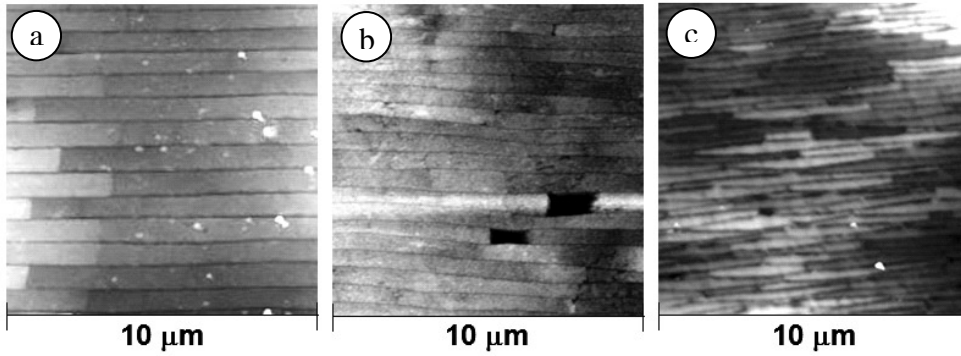
Figure 2: Scanning probe microscopy images (tapping mode) of (a) Top shell; (b) Pen Shell; (c): Pearl Oyster.

3 The deformation of nacre

Nacre from Red Abalone (RA), Top Shell (TS), Pen Shell (PS) and Pearl Oyster (PO) were deformed up to failure in quasi-static conditions (2 μm/sec) using a four point bending setup. Digital image correlation was used to measure the strains on the tensile and compressive faces of the sample (the strains always showed a linear progression with distance across the sample). The magnitudes of the tensile and compressive strains were initially identical. However upon reaching a critical load the material started to yield in tension and the strain on the tensile face became greater in magnitude compared to the compressive face (the neutral axis therefore shifted towards the compressive face). All samples failed by tensile failure of the material. Using basic equilibrium relations in the specimen, the compressive and tensile response of the material can be found using the deconvolution equations [4, 18]:

Tensile stress-strain curve : $\sigma(\varepsilon_t) = \dfrac{1}{(\varepsilon_t - \varepsilon_c)BH^2} \dfrac{d\varepsilon_c}{d\varepsilon_t} \dfrac{d}{d\varepsilon_c}\left[M(\varepsilon_t - \varepsilon_c)^2\right]$

Compressive stress-strain curve : $\sigma(\varepsilon_c) = \dfrac{d\varepsilon_t}{d\varepsilon_c}\sigma(\varepsilon_t)$

The stress-strain curves computed from this technique are shown on figure 3b. All nacres showed a modulus of 50-60 GPa. The compressive behavior was linear up to the failure of the samples, whereas the tensile behavior showed inelastic strains accumulating at a tensile stress of 50-60 MPa. These strains can be explained by the tablet sliding mechanism (Figure 1b). The stress-strain curves for RA, TS and PS showed homogeneous deformations along the specimen gage and strain hardening up to failure at strains ranging from 0.5 to 1%. On the other hand, PO showed a maximum stress and a continuous softening up to failure at strains exceeding 1.5%. This softening behavior is the indication of localization of deformation. Digital image correlation indeed captured a localization of deformation at about 45° from the axis of the sample, which upon closer examination appear to be a crack, propagating across the sample in a stable fashion.
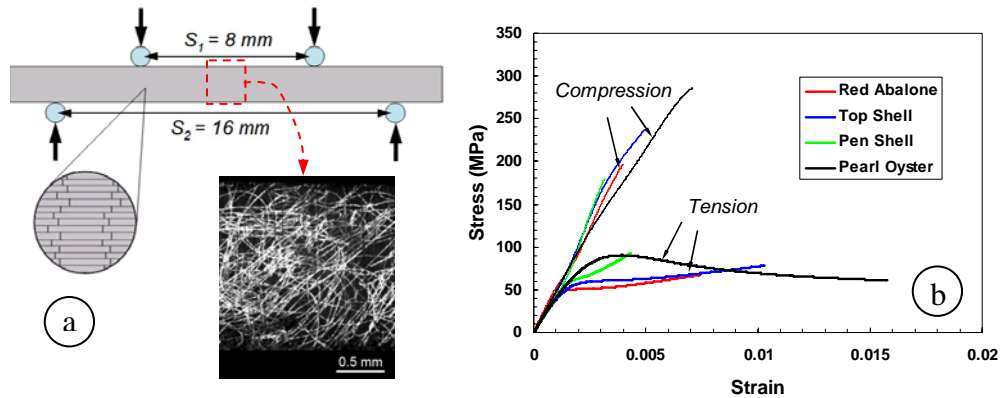
Figure 3: (a) four point bending setup showing microstructure orientation and surface preparation for digital image correlation; (b): Tensile and compressive behavior of four types of nacre

4 The fracture of nacre

Fracture experiments were performed using the same samples as for four-point bending, with the addition of a sharp notch on the tensile face of the sample. A pre-notch was produced by an initial diamond saw cut, which was then sharpened using a fresh razor blade. PS samples were the most difficult to handle because of their small size, and for those the notch was introduced with a razor blade directly. The dimensions of the specimen and the depth of the notch were chosen according to ASTM standard for fracture of ductile materials [19] (the size of the inelastic region being expected to be significant compared to the size of the specimen). A four point bending configuration was chosen in this work in order to enable microstructure-induced crack deflection. The specimens were coarsely

polished down to 9 micron diamond slurry. This enabled the monitoring of crack growth and of the inelastic regions. Figure 4 shows typical sequences of fracture for the four nacres tested.
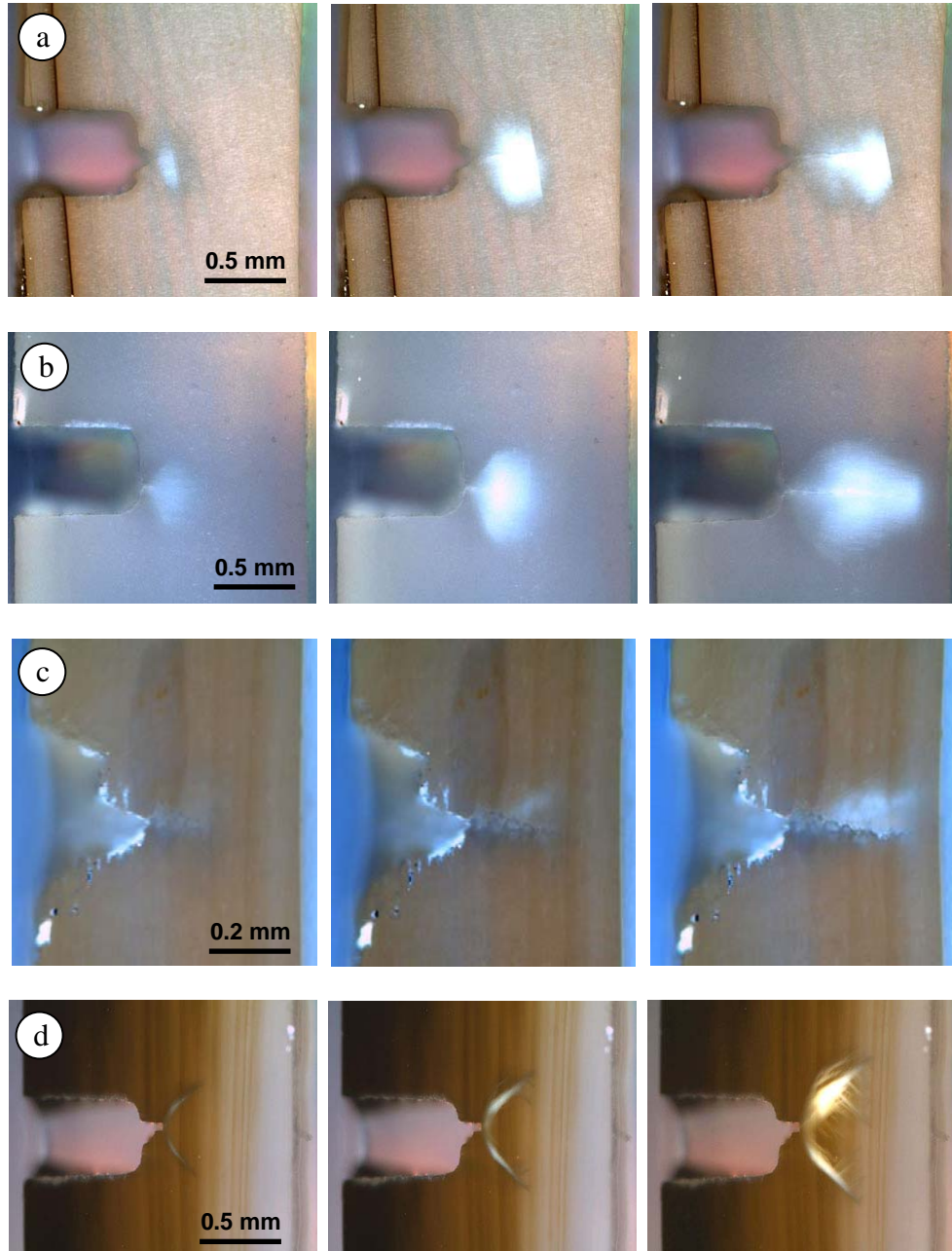
Figure 4: Snapshots taken during fracture tests for (a) Red abalone; (b) Top Shell; (c): Pen Shell; (d) Pearl Oyster.

All nacres showed some inelastic deformation ahead and behind the crack tip, manifested by whitening. Tablets being pulled apart expose molecular ligaments of organic materials, which scatter light and whiten the materials (in some polymers stress whitening is generated by the same optical phenomenon of light scattered by molecular chains in crazes). The deformation mode within these inelastic regions is tablet sliding, which dissipates a significant amount of energy via viscoplastic deformation of the interfaces. The energy dissipated in this process is significant and was recently showed to be one of the main sources of toughening for nacre [20]. Figure 4 shows that this inelastic region varied in size and shape from species to species. The initial inelastic region in top shell and red abalone was essentially round and about 0.4 mm (RA) and 0.5 mm (TS) in diameter. Crack propagation was very stable, leaving a wake of inelastic deformation. For RA the growth lines appeared to confine the inelastic region, and possibly impeded crack propagation. The inelastic region in pen shell was comparatively small in size (Figure 4c). The most surprising inelastic pattern was observed in PO nacre (Figure 4d): That material developed two distinct narrow bands at about +/- 45º from the crack line, reminiscent of shear bands in metals. The crack then propagated through one of these branches, possibly because of higher damage in these areas. Upon propagation the crack developed secondary narrow branches, forming a tree-like pattern. Further microscopy is currently under way to elucidate the exact deformation and fracture mechanisms in these branches. The extension of the crack was measured from the optical images, and toughness was computed using fracture standards [19]. The crack-resistance curve was thus established for all four nacres (Figure 5).
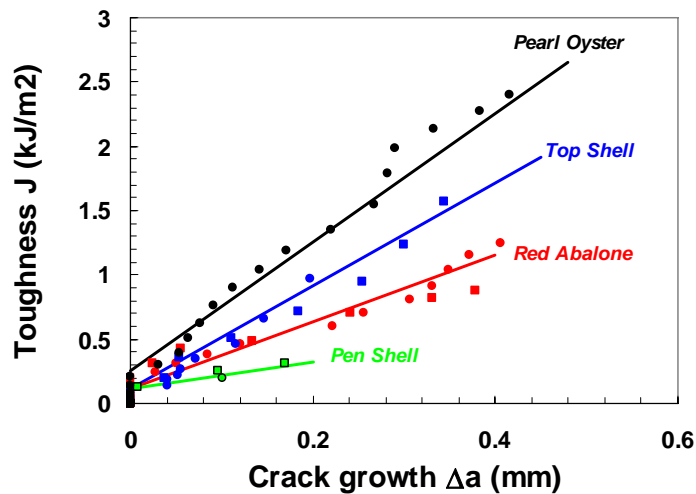
Figure 5: Crack resistance curve for the four types of nacre tested.

For all nacres crack propagated at toughness values of about 0.2 kJ/m^2. All nacres then showed increase in toughness with crack extension, but to different extents. PS was the most fragile and pearl oyster was the toughest, with a sharp rising crack resistance curve and a maximum toughness of 2.5 kJ/m^2. RA and TS were

between PS and PO in terms of toughness. Note that a rising crack resistance curve is essential to the stabilization of micro-cracks with in the material and as such it is a critical ingredient in the damage tolerance and reliability. The toughness of the four nacre tested also seem to correlate with the size of the inelastic region, which suggests that the energy dissipated in those region is an important contributor to toughness in nacre.

5 Conclusions

Nacre is a high performance natural material which provides a biomimetic model for novel engineering materials. While it is often proposed that the microstructure of nacre optimizes toughness, actual observation reveal significant differences of structures from species to species, which suggest that there could be several optima. Attempts to mimic nacre have so far not been entirely successful, which can be partially explained by a lack of microstructure design and optimization. In an effort to gain more insight in the design guidelines behind nacre, four types of nacre were characterized in this work. All nacres showed nonlinear deformation in tension along the tablets, with similar moduli (E=50-60 GPa) and strengths (50-60 MPa). All nacres also showed strain hardening in tension except Pearl Oyster which showed localization, yet still relatively high strains at failure. All nacres developed inelastic regions, to different extents, ahead of the crack tip. The size of these inelastic regions correlated well with the measured toughness. Cracks in Red Abalone showed some interaction with growth lines. Nacre from Pearl Oyster was found to be the toughest; it also had a unique pattern of inelastic deformations and fracture. Current work includes in-situ mechanical tests at larger magnifications in order to monitor the evolution of the microstructures ahead and behind the crack. Microstructure-based numerical models are also in development. Combinations of experimental observations and modeling are expected to elucidate the different toughening mechanisms operating in nacre across species.

References

[1] F. Barthelat, Biomimetics for next generation materials, Philosophical Transactions of the Royal Society a-Mathematical Physical and Engineering Sciences 365 (2007) 2907-2919.
[2] A. P. Jackson, J. F. V. Vincent and R. M. Turner, The Mechanical Design of Nacre, Proceedings of the Royal Society of London (1277) 234 (1988) 415-440.

[3] B. L. Smith, T. E. Schaeffer, M. Viani, J. B. Thompson, N. A. Frederick, J. Kindt, A. Belcher, G. D. Stucky, D. E. Morse and P. K. Hansma, Molecular mechanistic origin of the toughness of natural adhesives, fibres and composites, Nature (London) (6738) 399 (1999) 761-763.

[4] R. Z. Wang, Z. Suo, A. G. Evans, N. Yao and I. A. Aksay, Deformation mechanisms in nacre, Journal of Materials Research 16 (2001) 2485-2493.

[5] B. J. F. Bruet, H. J. Qi, M. C. Boyce, R. Panas, K. Tai, L. Frick and C. Ortiz, Nanoscale morphology and indentation of individual nacre tablets from the gastropod mollusc Trochus niloticus, Journal of Materials Research (9) 20 (2005) 2400-2419.

[6] F. Barthelat, H. Tang, P. D. Zavattieri, C. M. Li and H. D. Espinosa, On the mechanics of mother-of-pearl: A key feature in the material hierarchical structure, Journal of the Mechanics and Physics of Solids (2) 55 (2007) 225-444.

[7] F. Song and Y. L. Bai, Effects of nanostructures on the fracture strength of the interfaces in nacre, Journal of Materials Research 18 (2003) 1741-1744.

[8] X. D. Li, W. C. Chang, Y. J. Chao, R. Z. Wang and M. Chang, Nanoscale structural and mechanical characterization of a natural nanocomposite material: The shell of red abalone, Nano Letters (4) 4 (2004) 613-617.

[9] M. Rousseau, E. Lopez, P. Stempfle, M. Brendle, L. Franke, A. Guette, R. Naslain and X. Bourrat, Multiscale structure of sheet nacre, Biomaterials (31) 26 (2005) 6254-6262.

[10] G. Mayer, Rigid Biological Systems as Models for Synthetic Composites Science (5751) 310 (2005) 1144-1147.

[11] W. J. Clegg, K. Kendall, N. M. Alford, T. W. Button and J. D. Birchall, A Simple Way to Make Tough Ceramics, Nature (6292) 347 (1990) 455-457.

[12] Z. Y. Tang, N. A. Kotov, S. Magonov and B. Ozturk, Nanostructured artificial nacre, Nature Materials (6) 2 (2003) 413-U418.

[13] S. Deville, E. Saiz, R. K. Nalla and A. P. Tomsia, Freezing as a path to build complex composites, Science (5760) 311 (2006) 515-518.

[14] L. J. Bonderer, A. R. Studart and L. J. Gauckler, Bioinspired design and assembly of platelet reinforced polymer films, Science (5866) 319 (2008) 1069-1073.

[15] H. J. Gao, B. H. Ji, I. L. Jager, E. Arzt and P. Fratzl, Materials become insensitive to flaws at nanoscale: Lessons from nature, Proceedings of the National Academy of Sciences of the United States of America (10) 100 (2003) 5597-5600.

[16] J. D. Currey, Mechanical Properties of Mother of Pearl in Tension, Proceedings of the Royal Society of London (1125) 196 (1977) 443-463.

[17] W. H. Peters and W. F. Ranson, Digital imaging techniques in experimental stress analysis, Optical Engineering (3) 21 (1982) 427-431.

[18] Y. Sugimura, J. Meyer, M. Y. He, H. Bartsmith, J. Grenstedt and A. G. Evans, On the mechanical performance of closed cell Al alloy foams, Acta Materialia (12) 45 (1997) 5245-5259.

[19] ASTM standard E 1820-01: *"Standard Test Method for Measurement of Fracture Toughness"* (2004).

[20] F. Barthelat and H. D. Espinosa, An experimental investigation of deformation and fracture of nacre-mother of pearl, Experimental Mechanics (3) 47 (2007) 311-324.